Preliminary Inquiry into Spatial and Temporal Sensitivities while Conducted Near Shore Anti-Submarine Warfare (ASW)

LCDR Justin Reeves

17 September 2004

OC3570 Cruise Project

1. Introduction

The classic approach to solving the passive acoustic problem involves using the passive sonar equation. The equation is defined as:

$$SL - TL = NL - DI + DT$$

where SL represents the target's source level, TL represents the transmission loss the acoustic wave experiences through either cylindrical/spherical spreading or attenuation, NL represents the sum of ambient (or background) noise and the sensor's self noise (i.e. flow around the hydrophone), DI represents the directivity index and finally DT represents detection threshold. The left hand side numerically describes how a signal with a particular strength (SL) losses signal strength (i.e. intensity) through a combination of geometric spreading and attenuation. The right hand side numerically describes the level of background noise (NL), the ability of a sensor to discern a signal out of the background noise (DI) and the signal strength the sensor requires for detection (DT). A more basic definition of the passive sonar equation would be to say that this equality is satisfied when the desired acoustic signal is just detectable (i.e. equals) over the background noise. If the signal level were greater than the background noise, one would have a stronger level (or signal excess) than necessary to differentiate the signal out of the background noise. This is commonly referred to as Signal Excess (SE) and is easily solved for using the passive sonar equation. Simply rearrange the formula shown above so that all the variables are located on one side:

$$SE \equiv SL - TL - (NL - DI + DT)$$

Therefore, when SE is equal to zero, the signal is just detectable over the background noise. If SE > 0, the signal is easily detected over the background noise.

Some of the parameters described above are defined strictly by the design of the equipment. These parameters include Target Source Level (SL), Self Noise Level (NL), Receiving Directivity Index (DI) and the Detection Threshold (DT). Since these parameters are functions of equipment design only, their corresponding values are independent of where the sensor is placed and the length of time deployed. However, the remaining parameters, namely

Transmission Loss (TL) and Ambient Noise (AN), are impacted by the medium (i.e. ocean). The ocean is a fluid and dynamic medium whose physical properties are constantly changing from the ocean-basin level down to sub-mesoscale level. This paper will investigate how temporal and spatial changes within this medium of only a few hours and/or nautical miles can cause significant fluctuations in signal excess.

2. Measurements

Measurements for this analysis were made following the OC3570 2004 summer cruise on board the R/V Point Sur. Data was collected during three separate exercises that occurred from August 11th through the 13th. The data collected consisted of XBT launches, CTD (Conductivity, Temperature and Depth) casts and various meteorological parameters. Meteorological conditions were recorded on the underway data acquisition system (UDAS) as the ship maneuvered around the SCORE Range and time & position information of the R/V Point Sur was collected via GPS receivers. During all three exercises, SPAR buoys were launched from the stern of the R/V Point Sur. These SPAR Buoys were equipped with handheld GPS receivers and various combinations of sonobuoys. The sonobuoys used included the AN/SSQ-53E/F, AN/SSQ-57C and the AN-SSQ-77B. Various depth combinations were used and all buoys were used in either calibrated omni-direction (53’s and 57’s) or convergence zone (77’s only) mode. The sonobuoy acoustic data was transmitted via RF signal and was recorded onboard the R/V Point Sur. Sonobuoy data was digitized at approximately 40 Khz. Due to the over all length of all three exercises and the amount of data collected (over 24 GB), this paper will limit its discussion to the final exercise. Also used in this study was the Generalized Digital Environmental Model (GDEM) that provided monthly ocean profiles of salinity, temperature and sound speed based for a specified latitude and longitude.

3. Data Processing

All data recorded on the R/V Point Sur was processed and viewed graphically using MATLAB code. All figures (with the exception of the Ray Trace, Transmission Loss and Signal Excess plots) are a result of this processing. PC-IMAT v3.0 (UNCLAS) was used to generate the Ray Trace, Transmission Loss and Signal Excess figures. True performance characteristics of U.S. Navy sonobuoys are classified. To alleviate security concerns, a “dummy” or generic sonobuoy was created in PC-IMAT and was used to create the Signal Excess Plots. All calculations for sound speed were done using Mackenzie's (1981) empirical formula. For each CTD cast, temperature was recorded every 2 dbar. It was necessary to convert units from dbar to meters. A formula described by Saunders (1981) was used. Using P in decibars, the conversion to Z in meters is as follows:

$$Z = (1 - C_1)xP - C_2xP^2$$

Where:

$$C_1 \equiv (5.92 + 5.25x\sin^2(\phi)x10^{-3}; \phi \text{ is latitude}$$

$$C_2 \equiv 2.21x10^{-6}$$

4. Synopsis

During the final exercise, the winds were only 7 to 12 knots over the OPAREA. According to the Beaufort Scale, these wind should have produced 1 to 3 foot seas (sea state 2); however, because observed winds were out of the north and the OPAREA was located on the southern side of San Clemente Island, the seas were fetch limited and were rarely observed above 1 foot.

Both XBT and CTD casts indicated a strong negative sound speed gradient down to 100 meters. Below 100 meters, an equally strong positive sound speed gradient was found that extended to approximately 135 meters. Thus, a shallow secondary sound channel (SSC) was centered at approximately

100 meters. This SSC was present throughout the OPAREA. Below the SSC, the sound speed profile (SSP) maintained a negative gradient all the way to the ocean floor.

5. Discussion

a. Variations of Sound Speed in Time and Space

Because sound waves are refracted in the ocean, one of the first concerns of the acoustic oceanographer is determine the path the sound wave will follow and to determine whether or not the wave front will even reach the hydrophone/sensor. As the sound wave propagates, the wave front is refracted toward slower sound speeds. If the sound speed is a maximum at the surface and decreases all the way to the ocean bottom, the sound wave will be refracted toward the bottom of the ocean.

The speed at which sound waves propagate is dependent upon temperature, salinity and pressure. Using these measurable quantities, empirical formulas (such as Mackenzie (1981)) are used to calculate the speed of sound in water. Since the gradients of these quantities in the vertical are typically much stronger than gradients in the horizontal in the open ocean (with the exceptions of fronts and eddies), the acoustic oceanographer naturally is more interested in the vertical sound speed profile (SSP) than the horizontal plot of sound speed.

If in-situ measurements of these three oceanographic variables are not available, GDEM data is often used to calculate the SSP, however, because the GDEM is a climatological database, mesoscale and smaller scale temporal and spatial variations have been "averaged out". As expected, there were SSP features present in the XBT

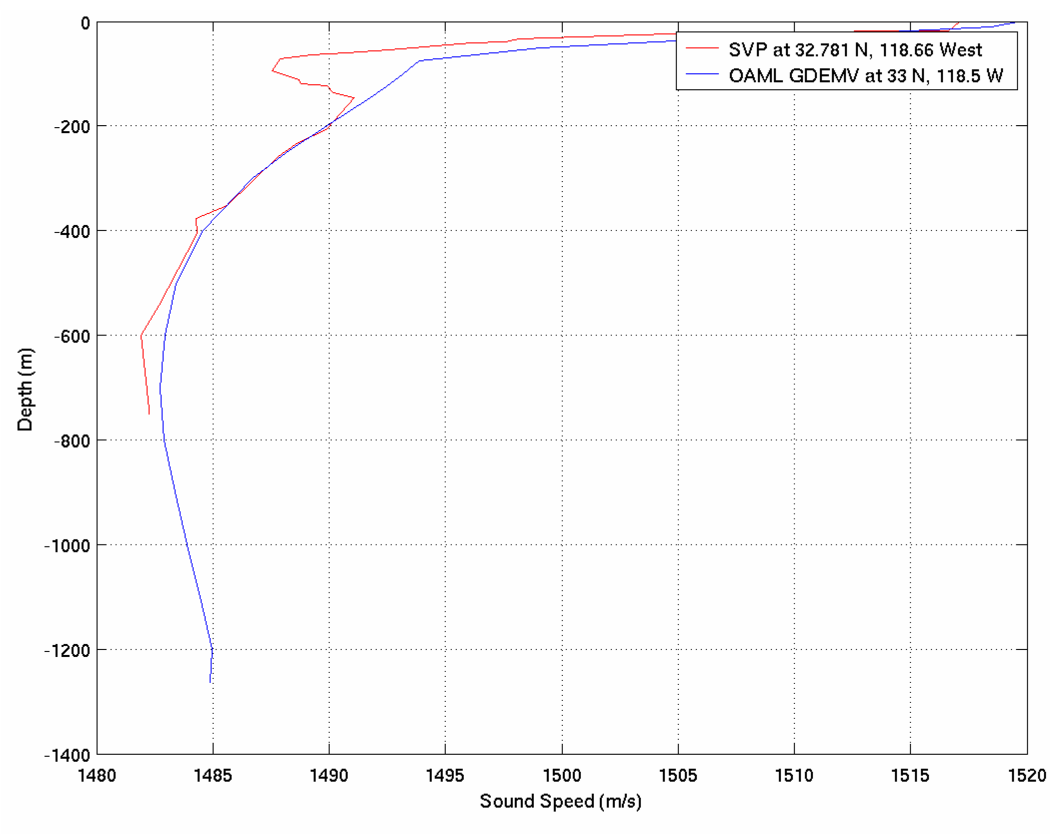

Figure 1

cast that the GDEM data clearly does not resolve (figure (1)).

Several studies have been completed by previous OC3570 students (Schmeiser (2000), Boedeker (2001), Roth (2001) and Fang (2002)), who have accomplished a statistical analysis of XBT measurements compared to CTD measurements. This statistical approach has been completed ad nauseam so the focus on this paper will be more qualitative than quantitative.

During the two-day exercise, numerous XBT launches were conducted; however, only during the last exercise was a CTD cast performed. From 0710Z to 1110Z on the 12th, a total of 5 XBT Probe launches were completed over the OPAREA during the final exercise as shown in figures (2)

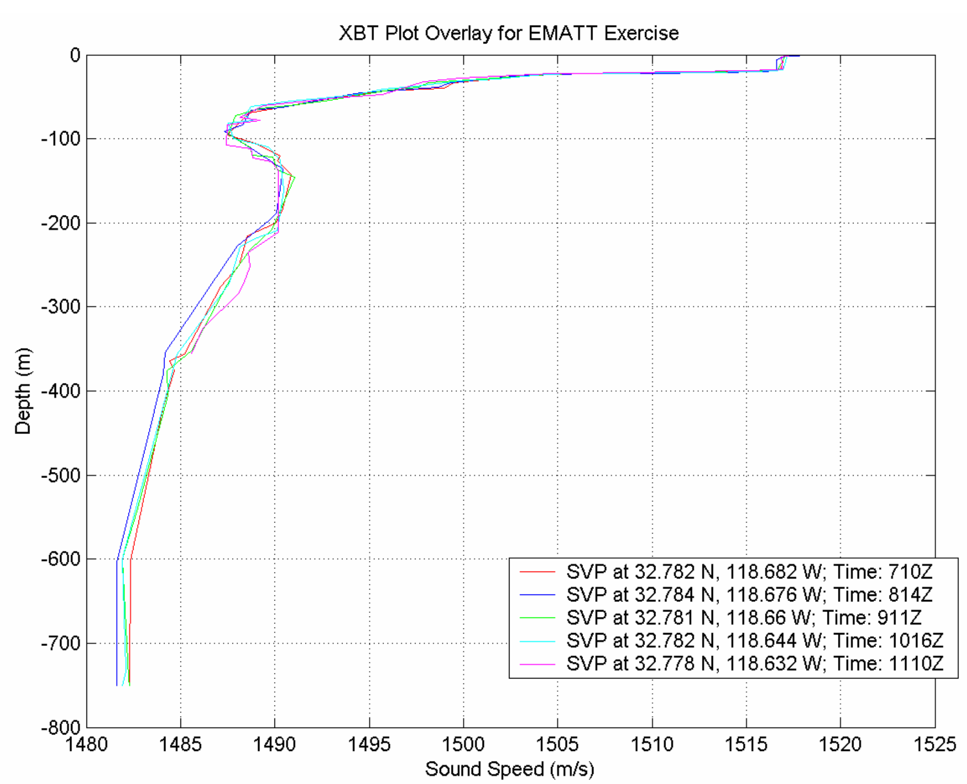

Figure 2

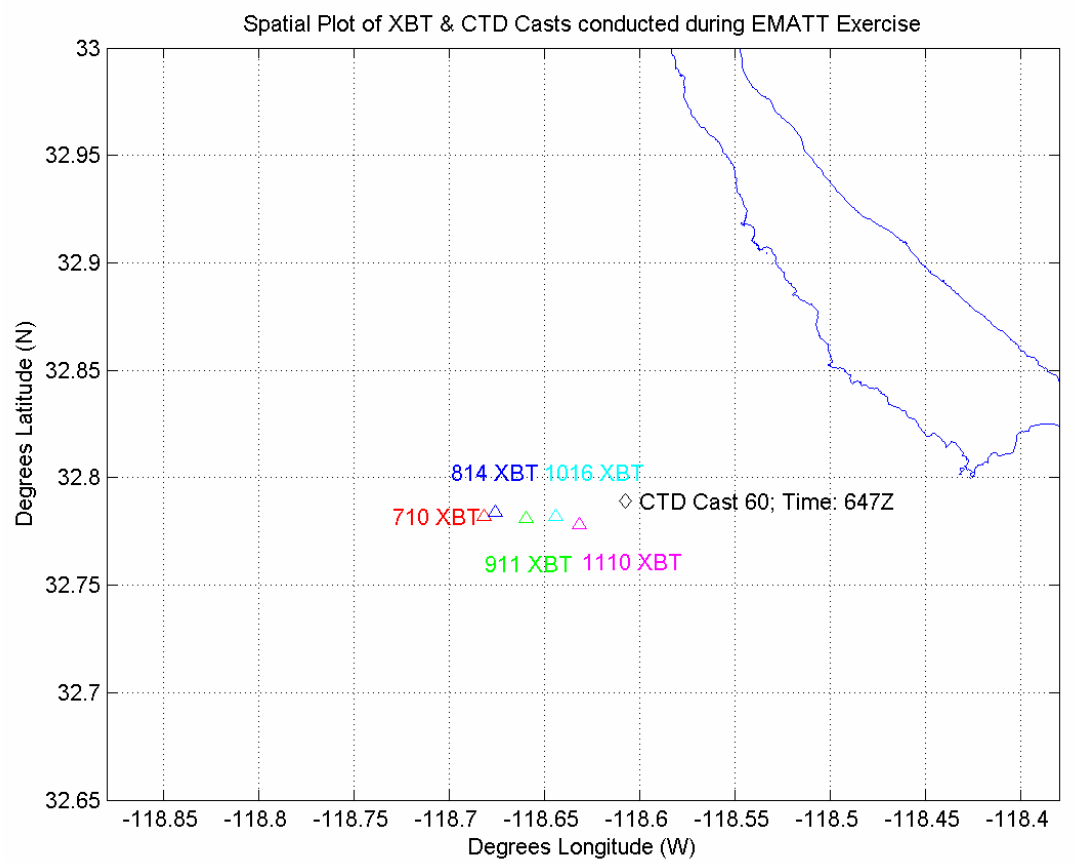

Figure 3

and (3). Approximately three nautical miles separated the position between the first probe launch and the final probe launch. All 5 launches showed very little variation in space and time, with the maximum difference between sound speed profiles of ~ 1 m/s.

Since XBTs cannot measure all three parameters directly (it measures temperature, but not salinity or pressure), a comparison was done between the XBT's estimated SSP and the SSP calculated by the CTD cast. Figure (4) depicts the oceanographic parameters measured by the XBT and CTD.

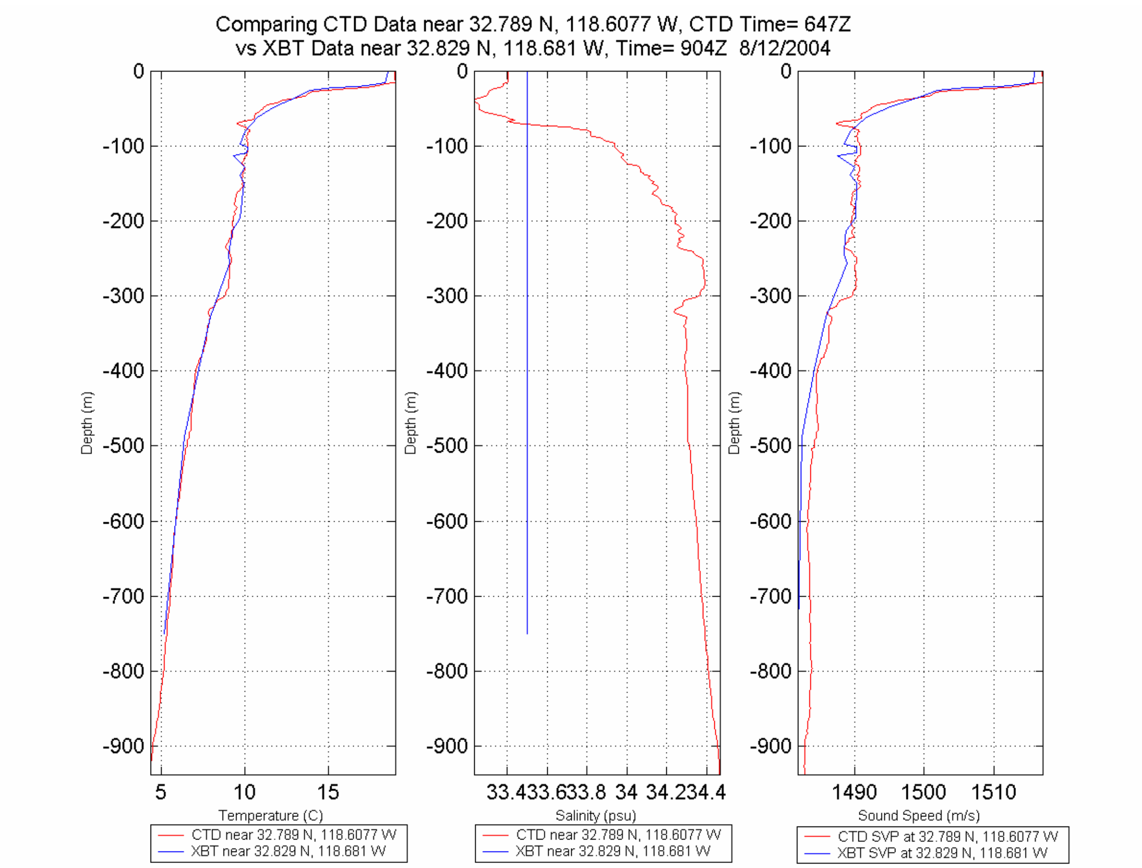

Figure 4

The XBT probe measures temperature and estimates depth based on an assumed "free fall" decent rate. Once the XBT cast is complete, an assumed salinity value (33.5 psu) is entered into MATLAB and the SSP was calculated via Mackenzie's equation (figure (4), right panel). Using the same formula, the CTD data was then used to calculate the SSP (figure (4) right panel). Although the two casts were not conducted at the exact same time or place (time and distance separation were approximately 2 ½ hours and 5 nautical miles respectively), the calculated SSP difference between the two methods was less than 3 m/s over the entire depth. Since sound waves travel ~1500 m/s (or ~ 1 nautical mile per second), one could infer that a 3 m/s difference would lead to a ± 30 meter error for every 10 nautical miles the sound wave travels. By order of magnitude comparison, this result is insignificant, even for naval Anti-Submarine Warfare (ASW) applications.

In this particular study, temporal and spatial changes of the SSP in the water column simply did not occur. The weather and oceanographic conditions around San Clemente were fairly benign. Intuitively, either strong mixing or river run off could lead to a spatially and temporally sensitive SSP. To quantify time/length scales, future projects may want to investigate changes within Monterey Bay. Strong winter storms that transition over Monterey Bay could lead to a rapidly changing SSP, as well as, periods when the Monterey Peninsula experiences sustained strong northerly winds, which would lead to enhanced upwelling. As coastal ASW is becoming more and more of a U.S. Navy priority, coastal areas near to where the Salinas River flows into the Monterey Bay should be investigated to determine the sensitivity of the SSP to fresh water inflow.

b. Spatial and Temporal Variations of Ambient Noise

For all three exercises, initial ambient noise values were determined using the Wentz Curve (figure (5)).

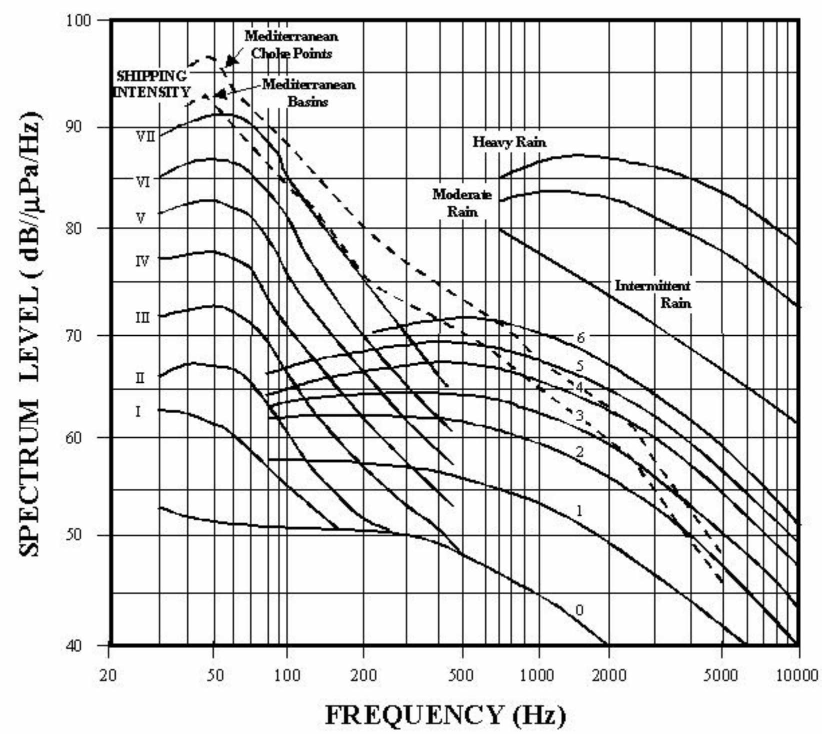

Sea State	Wind Speed (Kts)
6	28 - 47
5	22 - 27
4	17 - 21
3	11 - 16
2	7 - 10
1	4 - 6
0	1 - 3

Figure 5 (Wentz Curve)

Noticeably, the intensity level (dB) and source of ambient noise is dependent upon frequency. During the final exercise, two Expendable Mobile ASW Training Targets (EMATTs) were used as a sound sources. The pre-programmed frequencies were 400 and 900 Hz; consequently, the discussion will focus on 400 and 900 Hz as the primary frequencies of interest. As can be seen from figure (5), the 900 Hz was primarily affected by sea state, while both distant shipping and sea state impacted 400 Hz. Based off of the shipping density chart (figure (6)) and the UDAS measured wind speed (figure (7)), static ambient noise estimates values for 400 and 900 Hz were 65 dB and 61 dB, respectively.

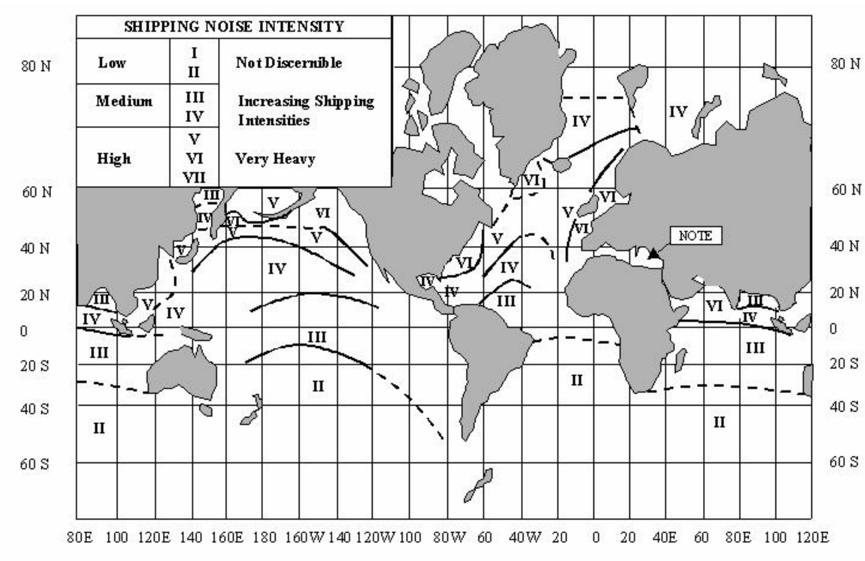

Figure 6

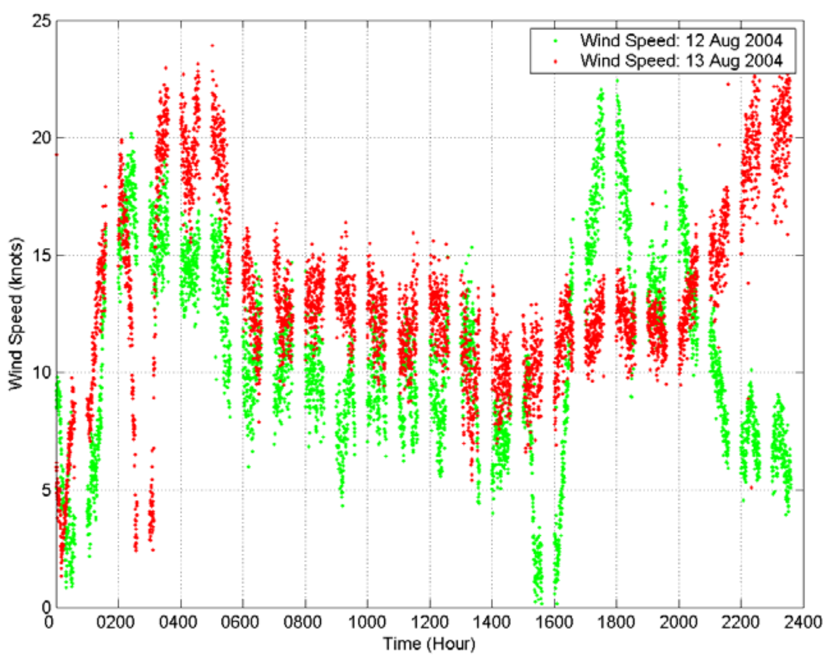

Figure 7

From the Wentz curve estimates, these values were considered as non-varying constants, but is that a truly accurate measurement of ambient noise?

In situ ambient noise measurements were obtained with the sonobuoys. A power spectrum density estimate via Welch's method was used to convert the digitized sonobuoy data (measured in volts) of both measurements into a power spectral density value (dB/Hz). Once the power spectrum density was calculated for each frequency, the sonobuoy frequency response envelope (not shown) was then used to calculate the final ambient noise value.

A random data sample was used to compare in situ measurements against the Wentz’s curve estimates. The data sample was viewed on a spectrogram for indication of radio frequency interference (RFI). Once no indications of RFI were found, the data sample was scrutinized audibly for possible RFI or other contamination. A 10 second sound byte was used to generate the power spectrum density.

The first random sample's power spectrum density is shown in figure (8).

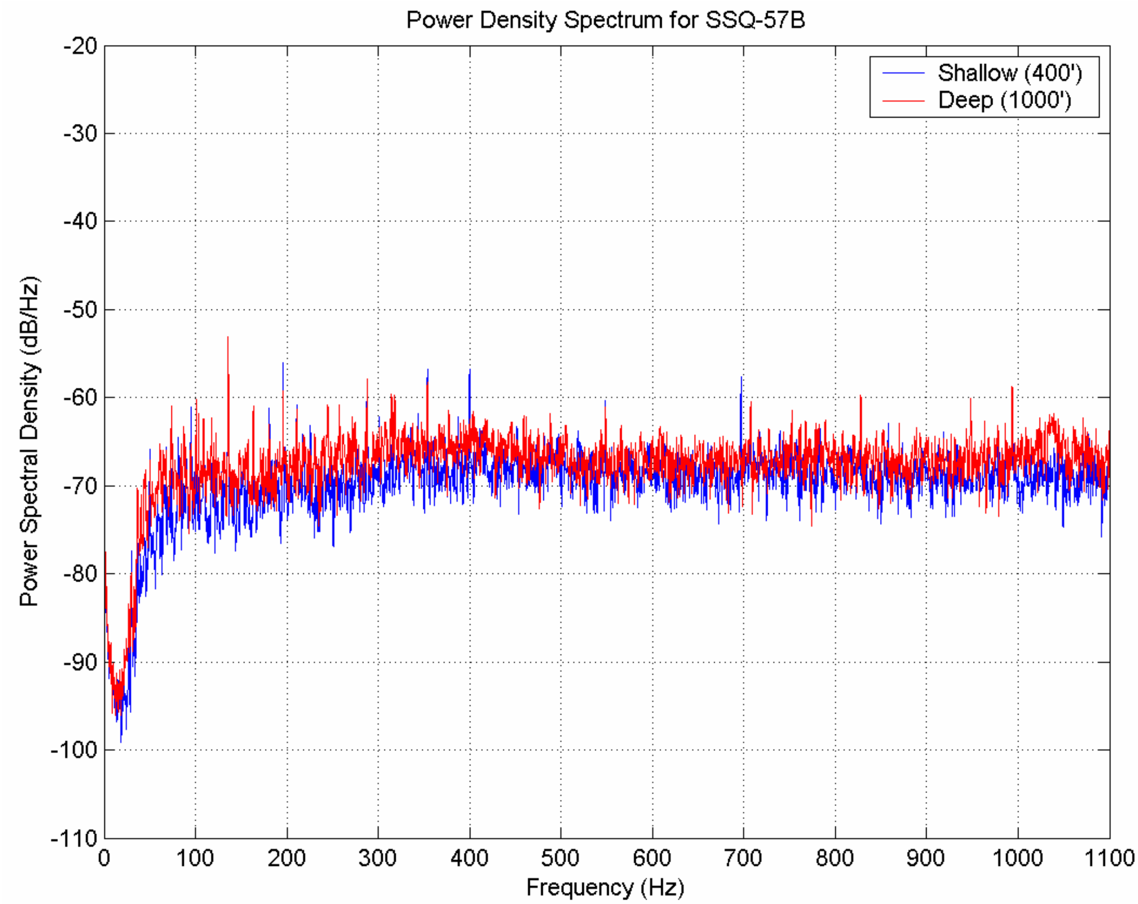

Figure 8

The data originated from two co-located sonobuoy sensors. One sensor was placed at 400 feet, the other at 1000 ft. The two different hydrophone depths were plotted against each other to error check the data. Once the sonobuoy frequency response envelope was applied to the power spectrum density, in situ ambient noise values were found to be 56 and 61 dB for 400 and 900 Hz respectively. Although the Wentz curve ambient noise estimates in the 400

Hz bandwidth were not very realistic when compared to in-situ data, the 900 Hz estimate was extremely accurate. Was this just a lucky selection, or are ambient noise estimates via the Wentz curve fairly accurate?

To test this hypothesis, two more data samples were chosen at random. To minimize errors resulting from difference in sensor performance, the analyzed data came from the same sonobuoy. The data was error checked using the same method as described above. The measurements varied by over three hours and, because of the northwestward set, the buoys drifted slightly in space as well (~.58 nautical miles). Figure (9) is the power spectrum density plot for the two samples.

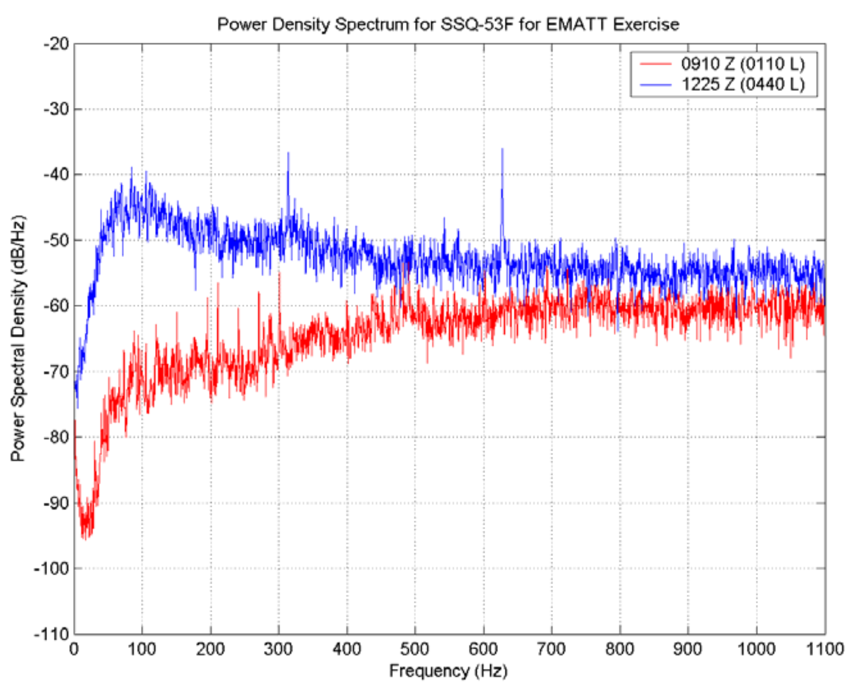

Figure 9

Figure (9) visibly demonstrates the strong temporal and presumably spatial variation of ambient noise. Over a three-hour span, 400 Hz increased by 13 dB and 900 Hz increased by 6 dB. To ensure that the increase in the lower frequencies were not associated with R/V Point Sur's noise, a comparison of the ship's position with respect to the ambient noise buoy (not shown) indicated that the increase occurred when the ship was further from the buoy/hydrophone. Therefore, it appears that the increase in ambient noise was caused by an increase in background noise and did not result from the ship self-generated noise from the R/V Point Sur. The final in situ measurements were observed to range from 59 dB and 72 dB for 400 Hz band and from 69 dB to 75 dB for the 900 Hz band.

Because of time constraints, a complete temporal analysis of all the sonobuoy data was not completed. That would encompass analyzing approximately 9 GB of data for the last exercise alone. Further analysis could be done to look for a maximum separation between periods, but that would be extremely time consuming. Perhaps in future experiments, data could be recorded as a power spectrum density plot with respect to time (i.e. every minute, a PSD is performed and recorded). These curves could be more efficiently analyzed for maximum separations.

c. Impact to Signal Excess

Since the SSP was invariant during the final exercise, fluctuating sound paths and its impact to signal excess cannot be qualitatively evaluated. However, the temporally sensitive, in situ ambient noise values can be utilized to produce qualitative results that can be evaluated.

Figure (10) is a ray trace based on the SSPs calculated during the last exercise. This figure demonstrates how a finite number of possible sound waves (at various incident angles) will be refracted in the water column and the possible paths these sound waves may take.

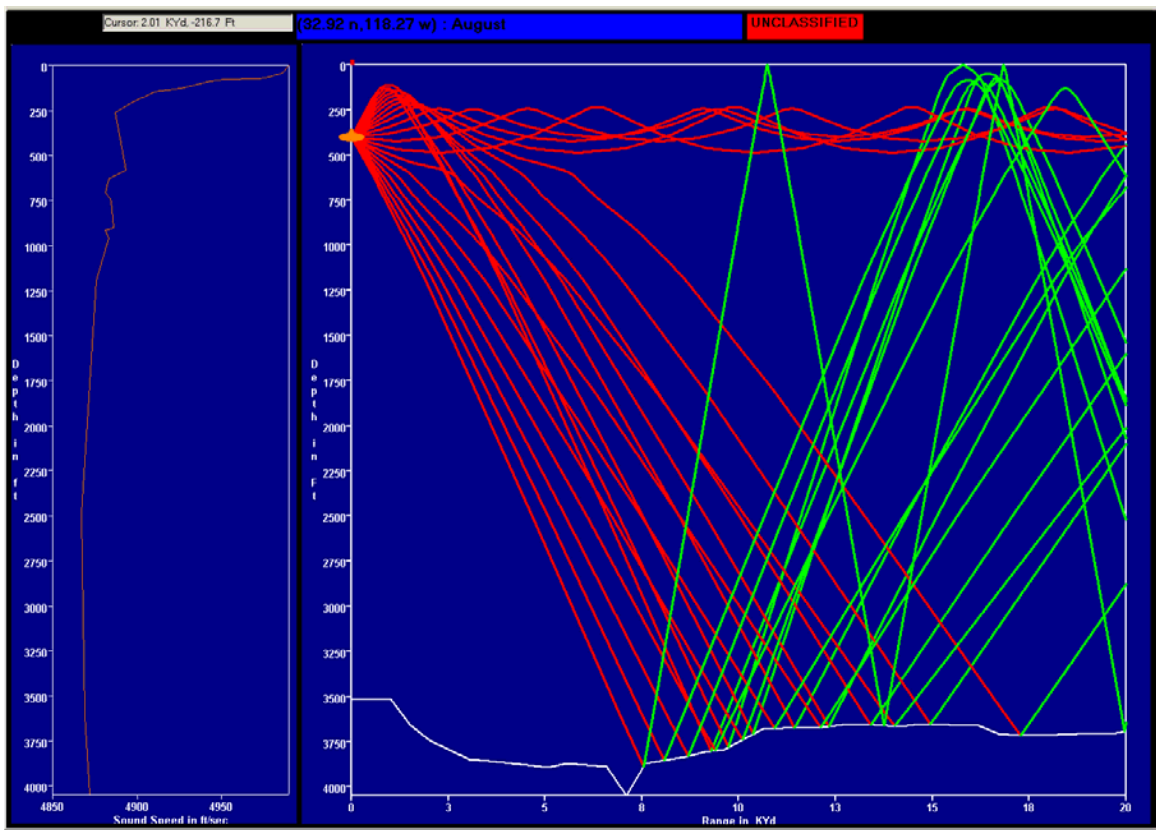

Figure 10 (Ray trace for target in secondary sound channel)

The ray trace shows a secondary sound channel located at approximately 100 meters in depth. This channel may help to focus sound waves along its axis if the sound source is transmitting within it. Otherwise, the ray trace indicates that most energy is being refracted away from the surface and driven into the bottom.

As discussed previously, Signal Excess (SE) occurs when the signal level exceeds the background noise and it is possible to differentiate the signal from the background noise. By adding ambient/background noise, it becomes more difficult for the sensor (or operator) to distinguish the signal from the background noise. To demonstrate this, Signal Excess plots were created using PC-IMAT. Again, because of security concerns, these plots represent qualitative results and should not be inferred as quantitative measurements of actual sensor performance. Although Signal Excess plots were computed for both 400 Hz and 900 Hz, this section will focus on 400 Hz due to the larger variation in intensities between ambient noise measurements.

Utilizing PC-IMAT, the Signal Excess Sonar equation was solved graphically. A source level (SL) of 134 dB was assumed; directivity index and detection threshold were set to zero; PC-IMAT calculated the transmission loss.

Sonobuoy position was known as well as sensor depth. The only unknown was target depth. Figure (11) was calculated using the lower of the two ambient noise measurements (59 dB). Figure (12) was calculated using the exact same values entered into the sonar equation with the exception of the +13 dB higher ambient noise value (72 dB).

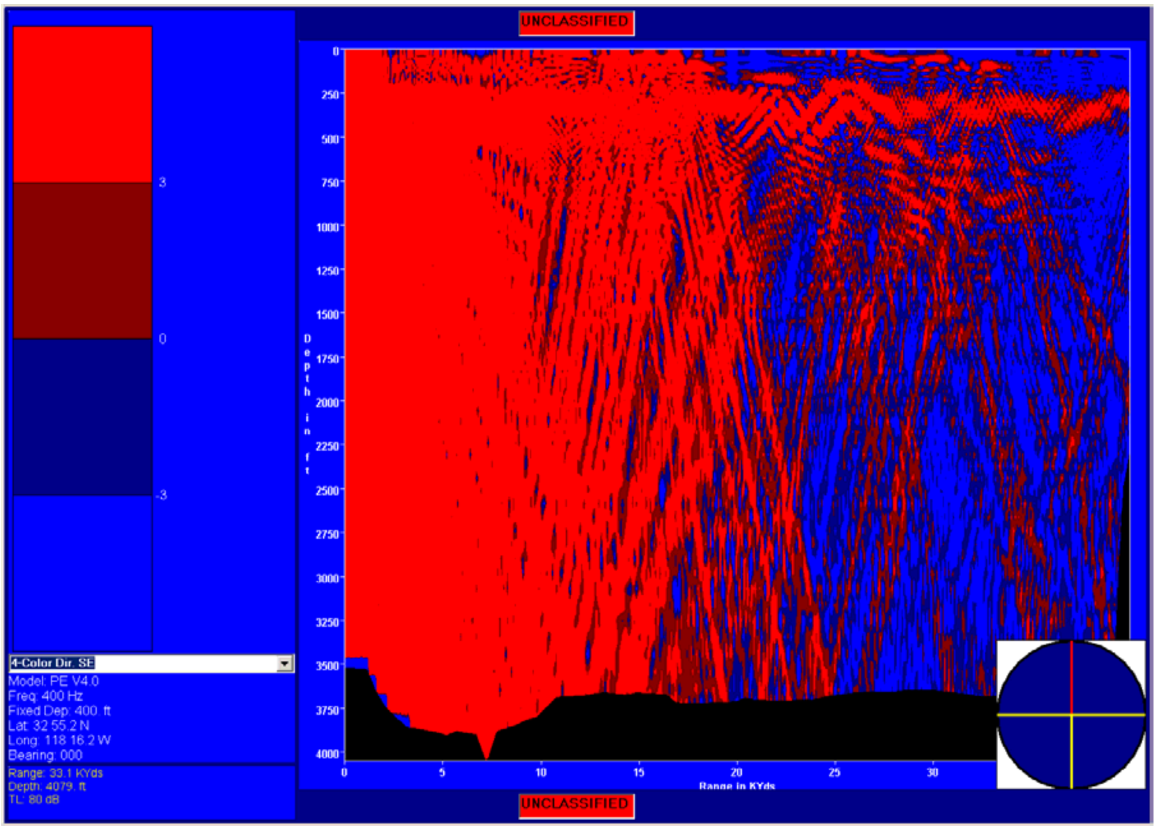

Figure 11 (400 Hz Signal; AN = 59 dB)

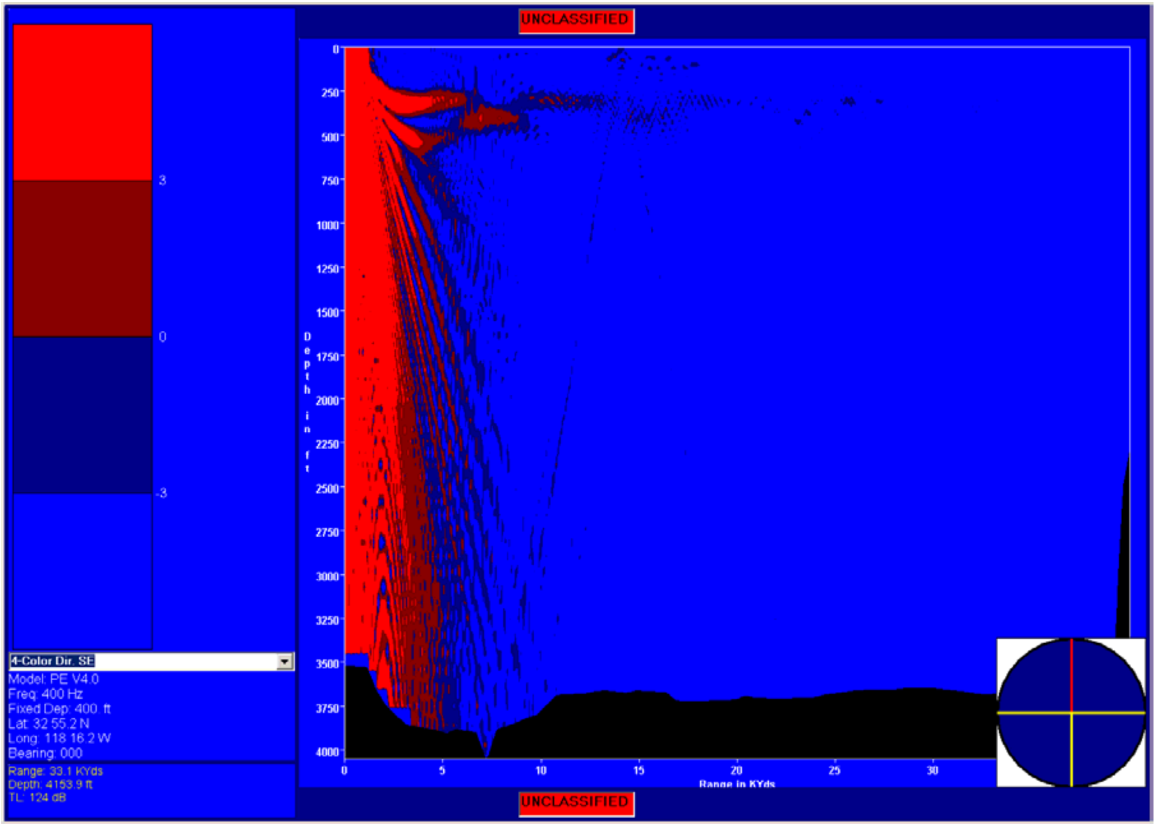

Figure 12 (400 Hz; AN = 72 dB)

As expected, the Signal Excess plot with the lower ambient noise value indicates that a signal can be detected at a significantly greater distance. As the ambient noise level increased, identifying the desired signal from the background noise becomes increasingly difficult; consequently, one would expect the detection range to decrease. Figures (11) and (12) were calculated placing the hydrophone at 400 feet. Setting the depth to 400 feet would place the hydrophone in the secondary sound channel. This would be the optimum placement and would yield the greatest detection range if the target was also located in the secondary sound channel. For example, looking at figure (12), if the EMATT was operating at 400 foot depth, the detection range (signal excess > 0) would be between 10,000 and 15,000 yards; however, if the EMATT was operating at only 100 feet, the detection range would decrease to approximately 1,500 yards. Looking at figures (11) and (12), a simple order of magnitude comparison shows that a target can be detected almost continuously out to 40,000 yards when the ambient noise value was around 59 dB; however, this detection range is decreased to less than 8,000 yards (target is not operating in secondary sound channel) when the ambient noise was increased to 72 dB. In other words, the detection range decreased by approximately 500%!

d. Experiment Results

During the final exercise, two EMATTs were launched from the R/V Point Sur. The first EMATT was programmed to emit at 400 Hz and the second was programmed to emit at 900 Hz. Three SPAR buoys were launched (labeled: blue, orange, and red) and were oriented along an east-west axis. On two of the SPAR buoys, the sonobuoys were set to 1000 feet; however, on the last buoy (red), the sonobuoy was set to 400 feet. The 400 Hz EMATT was programmed to follow an east-west racetrack pattern around the three SPAR buoys;

while the 900 Hz EMATT was to run a north-south racetrack pattern along the west edge of the SPAR buoys.

Two major problems were experienced during the exercise. First, tracking the 400 Hz EMATT in real-time on any of the buoys proved extremely difficult. Figure (13) is a spectrogram plot of the three sonobuoys observed at 0913Z. The blue and orange buoy show a pronounced 900 Hz signal, as well as, the faint 400 Hz signal (found at 40 - 52 seconds and 14 - 26 seconds, respectively). This figure demonstrates how signal excess can vary in space. Figure

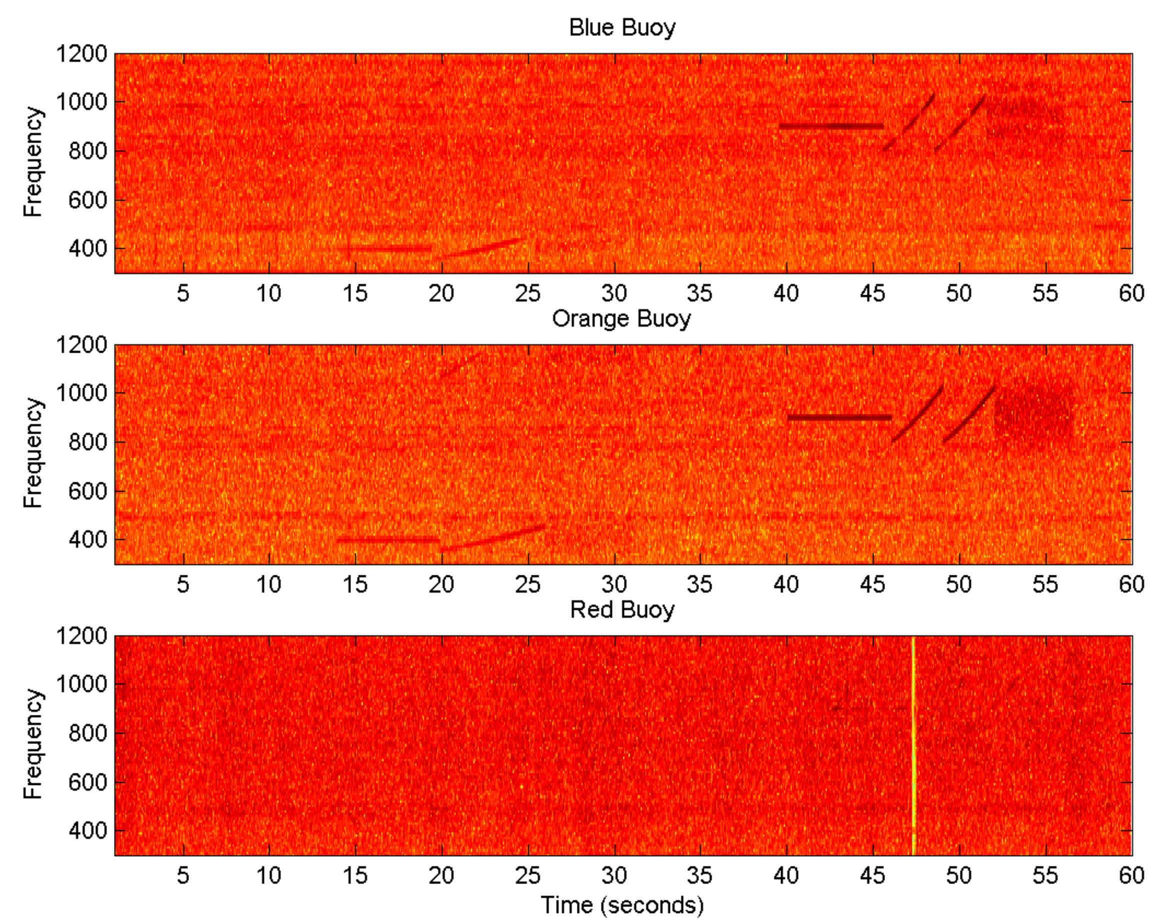

Figure 13 (Spectrogram for all three buoys at time 0913Z)

(14) is another spectrogram plot, but instead of showing the spatial dependence of signal excess, it displays the temporal changes observed on the blue buoy (hydrophone placement was deep).

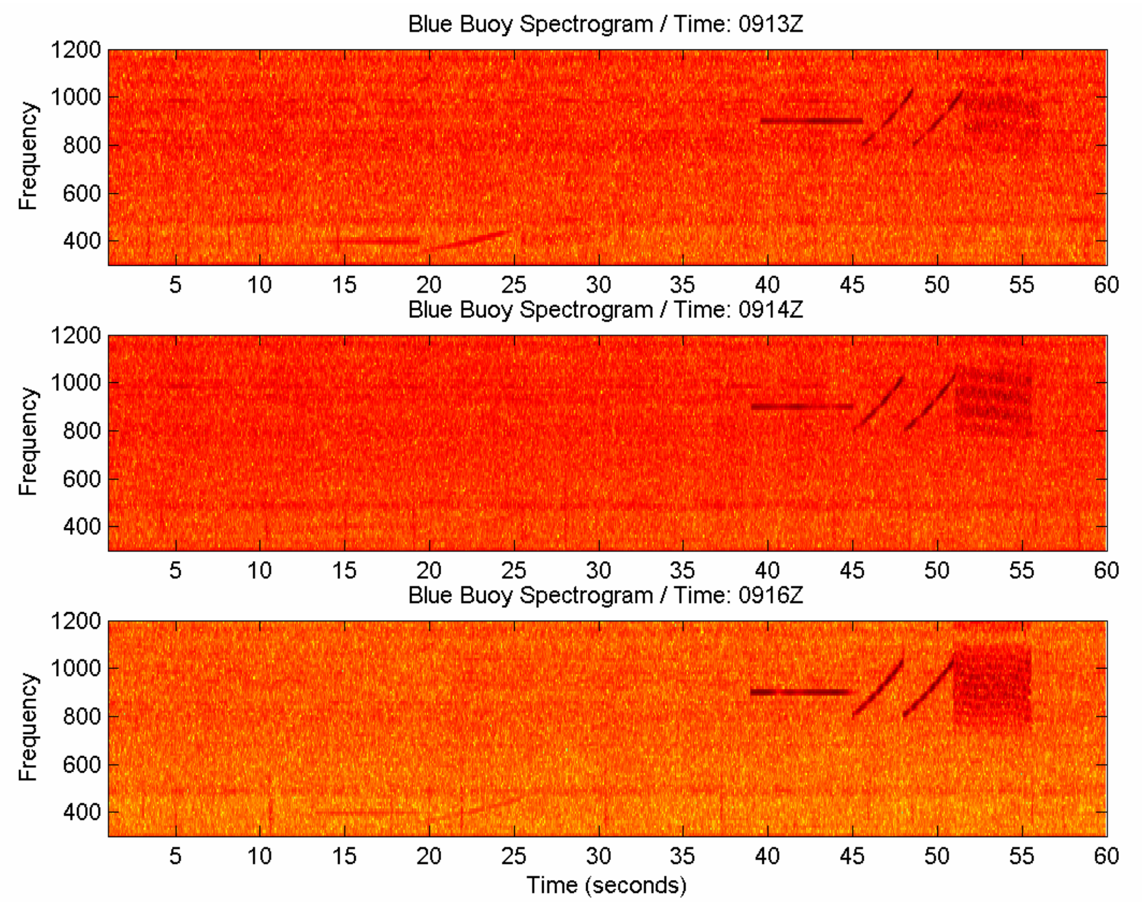

Figure 14

The 400 Hz signal transitions from contact held at 0913Z, then fades out. The target is not re-acquired for three minutes. The second problem noticed during the exercise was the red buoy almost never had contact with either EMATT. The 900 Hz EMATT was detected only three times on the red buoy, while the 400 Hz signal was never detected.

In the post analysis, both problems can be explained with the qualitative results of this paper.

First, the low number of detections of the 400 Hz EMATT can be explained using the signal excess plots. As previously discussed, the 400 Hz bandwidth showed strong temporal changes in intensity. This would lead to a fluctuating signal excess level. Periodically the signal could be detected from the background noise, but at other times, it could not. However, the 900 Hz signal showed only a 6 dB variation, so it would be expected that this signal would show a consistent detection rate. This explanation fits exactly with what was observed in figure (14). The 900 Hz signal, once contact was made, was held consistently; however, the 400 Hz signal would only be detected intermittently.

Secondly, the ray trace and signal excess plots indicate that all sound energy will be driven toward the bottom; sound energy transmitted from the EMATT would be refracted downward and away from the surface. Consequently, a hydrophone placed closer to the surface would have a more difficult time detecting the signal when compared to a hydrophone placed at a deeper depth since all the sound energy would be refracted toward the deeper hydrophone. Therefore, it is believed that the low number of detections on the red buoy resulted from the downward refraction of sound energy in combination with the shallow placement of the hydrophone. As shown in figure (13), both the 400 Hz and 900 Hz signal were detectable on the deeper hydrophones (blue and orange), but the shallow hydrophone was unable to separate out the weak signal from the background noise.

6. Conclusions

With the mass proliferation of diesel submarines throughout the world, littoral ASW has become the primary threat to US Forces operating in the littoral environment. Unlike the deep, blue-water areas of the world's oceans, the littoral battlespace is a rapidly and constantly changing environment that must be continuously sampled and analyzed. As discussed above, these changes were not accurately modeled using traditional climatological databases. Future academic research should be guided toward conducting real-time monitoring of both ambient noise and sound speed parameters with a focus on establishing quantifiable and accurate predictive capabilities of these spatially and temporally sensitive properties.